HHS Public Access

Author manuscript

J Mater Sci Technol. Author manuscript; available in PMC 2017 September 01.

Published in final edited form as:

J Mater Sci Technol. 2016 September ; 32(9): 815–826. doi:10.1016/j.jmst.2015.12.018.

Bio-Adaption between Magnesium Alloy Stent and the Blood Vessel: A Review

Jun Ma[1,2], **Nan Zhao**[1,2], **Lexxus Betts**[1,2], and **Donghui Zhu**[1,2,*]

[1]Department of Chemical, Biological and Bioengineering, North Carolina Agricultural and Technical State University, Greensboro, NC, USA

[2]NSF Engineering Research Center-Revolutionizing Metallic Biomaterials, North Carolina Agricultural and Technical State University, Greensboro, NC, USA

Abstract

Biodegradable magnesium (Mg) alloy stents are the most promising next generation of bio-absorbable stents. In this article, we summarized the progresses on the *in vitro* studies, animal testing and clinical trials of biodegradable Mg alloy stents in the past decades. These exciting findings led us to propose the importance of the concept “bio-adaption” between the Mg alloy stent and the local tissue microenvironment after implantation. The healing responses of stented blood vessel can be generally described in three overlapping phases: inflammation, granulation and remodeling. The ideal bio-adaption of the Mg alloy stent, once implanted into the blood vessel, needs to be a reasonable function of the time and the space/dimension. First, a very slow degeneration of mechanical support is expected in the initial four months in order to provide sufficient mechanical support to the injured vessels. Although it is still arguable whether full mechanical support in stented lesions is mandatory during the first four months after implantation, it would certainly be a safety design parameter and a benchmark for regulatory evaluations based on the fact that there is insufficient human *in vivo* data available, especially the vessel wall mechanical properties during the healing/remodeling phase. Second, once the Mg alloy stent being degraded, the void space will be filled by the regenerated blood vessel tissues. The degradation of the Mg alloy stent should be 100% completed with no residues, and the degradation products (e.g., ions and hydrogen) will be helpful for the tissue reconstruction of the blood vessel. Toward this target, some future research perspectives are also discussed.

Keywords

Mg stent; Bio-adaptation; Vessel; Wound healing

1. Introduction

In the past decade, the evolution of biodegradable stents has become one of the biggest topics of discussion in health care. For years, stents have been implanted in the body permanently by a metal or plastic material used to facilitate with problem areas in the

*Corresponding author. Ph.D.; Tel.: +1 336 285 3669; Fax: +1 336 334 7904., dzhu@ncat.edu (D. Zhu).

arteries. Due to relocking or a process of a permanent stent becoming inactive, there is a high chance that the patient is not receiving the proper care needed for the area of their body that is in need of a stent. Scientists have also found that biodegradable metallic material for stents may be more beneficial in the body than permanent metal due to a problem causing agent called late stent thrombosis. Mg-based biodegradable material has the key advantage to reduce or even eliminate the late restenosis[1]. Besides, Mg has attracted most attention because of its role in many important biological functions and its biocompatibility[1]. Mg-based stents are tailored to benefit the body and allow cell proliferation. The main problem of Mg for stent application is its rather rapid biodegradation, which occurs in the form of corrosion. This rapid corrosion could lead to loss of mechanical integrity and release of high concentration of degradation products. The first biodegradable magnesium alloy stent was created by Biotronik, which was made from WE43[2]. The stent demonstrated good biocompatibility and clinical trial has shown very promising results[3]. However, no matter it is bare Mg-based stent or drug-coated Mg-based stent material both of them showed obviously late lumen size loss[4], which is most likely caused by the maladaptation between the stent material and vascular tissues. In this review, the bio-adaptation of the host to the Mg alloy stent material is discussed.

2. Progress on Mg-Based Stents

2.1. *In vitro* studies

In vitro studies provide preliminary knowledge about the mechanical properties, corrosion resistance, and biocompatibility of Mg-based alloys. The mechanical properties and corrosion resistance of different Mg-based alloy systems were summarized in a previous review[5]. Here, we focus on the research progress on biocompatibility of Mg-based alloys. The *in vitro* biocompatibility and hemocompatibility of Mg alloys used in stent application are summarized in Table 1.

Due to improvement in corrosion resistance and mechanical strength by adding rare earth element (REE)[12], especially radial strength[13,14], Mg-REE alloy series are widely explored in cardiovascular stent application. Recently, newly developed Mg–Y–Zn alloys, ZW21 and WZ21, with very fine grains (<10 μm) and high ductility (17%–20% uniform elongation), have been demonstrated as promising candidates for stent application[15]. *In vitro* biocompatibility tests showed that both WZ21 and ZW21 had concentration-dependent viability and metabolic activities. At low concentration, no significant differences were observed between the extracts of alloy groups and medium control group. However, at high concentration, compared to other alloys, such as WE43, WZ21 and ZW21 had a higher cytotoxicity[16].

Another series of Mg alloys investigated in cardiovascular stent application are Mg–Li–(Al)–(REE). In one study, the biocompatibility of Mg3.5Li, Mg8.5Li1Al, Mg3.5Li4Al2REE, Mg8.5Li, Mg3.5Li2Al2REE, and Mg8.5Li2Al2REE was explored. Except for Mg8.5Li2Al2REE, all other alloys showed good cell viability and hemolysis ratio. Interestingly, although Mg8.5Li2Al2REE exhibited poor biocompatibility and had high hemolysis ratio, the least adhered platelet was observed[8].

The biocompatibility of a series of Mg–Y–REE alloys was also studied by indirect method. The addictive of Y and REE showed strong inhibition of smooth muscle cell (SMC) proliferation but moderate reduction of SMC viability. In contrast, endothelial cells (EC) were viable and showed proliferation. Addition of zinc and manganese had negative effects on viability and proliferation of both EC and SMC[17]. WE42, composed of 4% Y, 2% REE, and 0.5% Zr, showed a longer clotting time and higher hemolysis ratio, compared to 316 L stainless steel and surface-treated WE42. The anti-coagulant property of WE42 relies on the binding of Mg^{2+} to extracellular Ca^{2+}, thus delaying platelet aggregation[18].

Some surface treatments were also explored to enhance the corrosion and biocompatibility property of Mg stent materials. Results showed that hydrofluoric acid (HF) treated Mg–Nd–Zn–Zr alloy had no significant difference in EC viability, compared with untreated Mg–Nd–Zn–Zr alloy, while HF-treated alloy showed better hemocompatibility, with lower hemolysis ratio and smaller adhered platelet number[7].

A double-layer coating system, composed of microarc oxidation/poly-L-lactic acid (MAO/PLLA) composite coating and paclitaxel (PTX) release controlling PLGA coating, was deposited on AZ81 to control the biocorrosion, drug release behavior and hemocompatibility. The drug release rate exhibited a nearly linear release profile without significant burst release, and MAO/PLLA and PLGA50/50(8% PTX) showed less adhered platelets, compared to 316 L stainless steel, indicating the double-layer-coated AZ81 has the potential for drug-eluting stent application[19].

A series of Mg–Ca alloys with various Ca contents, ranging from 0.4% to 2%, showed signs of decomposition after 24 h incubation, compared to HF-treated alloys. After day 10, colonization of alloy surface was only observed for SMC, not for EC[6]. This study showed that HF-treated Mg–Ca alloys exhibited good mechanical properties and degradation kinetics. However, the biocompatibility of HF-treated and untreated Mg–Ca alloys was not acceptable. The roles Ca plays in bone healing and formation indicated that Mg–Ca alloy might be more suitable for bone implants than cardiovascular stent application[6].

Both EC and SMC are involved in vascular regeneration and remodeling. Most of the current *in vitro* test methods do not consider the interaction between EC and SMC. Co-culture systems of EC and SMC can mimic real *in vivo* scenario more closely and provide more convincing biocompatibility data for Mg alloys; therefore, different co-culture systems might be a better choice for *in vitro* analysis.

2.2. Animal studies

Because of important roles of REEs in mechanical strength and corrosion resistance of Mg alloys, alloys used in animal studies are mostly composed of REE and other alloying elements. And the most widely used alloy is WE43 (Y 3.7%–4.3%, Zr 0.4%, REE 2.4%–4.4%). Besides WE43, AE21, Mg–Y–Zn series, MgCa, and AZ31B have also been investigated for stent applications. The detailed comparisons of animal tests on Mg alloys, such as inflammation score, injury score, and neointimal area, are summarized in Table 2.

AE21 (2%Al, 1% REE) is the first Mg alloy used in stent application. Implanted in carotid artery of domestic pigs, AE21 showed positive results during remodeling phase; however, due to early neointima formation, the lumen diameter was still narrow, compared to the reference. And the inflammation was closely related to the extent of injury[21].

Lekton Magic stent, made of WE43, was implanted into the coronary artery of minipigs. Four weeks later, the Mg group showed a higher minimum luminal diameter (MLD), compared to 316 L stainless steel stent, indicating that less neointima was formed for Mg group. After 2 months, MLD in control group almost remained unchanged, while Mg group had an increased MLD from week 4 to week 12, suggesting a positive remodeling[22]. Similarly, another study on Lekton Magic stent was conducted in both minipigs and domestic pigs. Mg stent started to show signs of degradation at day 28. And at day 28 and 3 months, neointimal formation was significantly less in Mg stent group, compared to 316 L stainless steel stent. No significant differences in injury and inflammation were observed in both groups. Therefore, the less neointima formation in Mg group was probably due to the disappearance of mechanical irritation during degradation[24].

Absorbable metal stent (AMS), another WE43 stent, showed larger luminal diameter and less neointimal formation after implantation into coronary arteries of Göttingen minipigs at both day 28 and day 56, compared to 316 L stainless steel. From day 28 to day 56, histological analysis revealed no significant differences in the number of macrophages and Ki-67 positive cells, while for 316 L stainless steel stent, at early time, a significant higher number of proliferating cells was observed. The less neointimal formation and larger MLD suggested the advantages of AMS stent over 316 L stainless steel stent[17]. Slottow et al. explored the biodegradation of AMS stent in porcine coronary arteries. From 28 days to 3 months, both minimal lumen diameter and maximum lumen diameter were enlarged. In addition, lumen loss and percentage of intimal hyperplasia were also reduced from 28 days to 3 months. These observations indicate that a positive remodeling occurred from day 28 to 3 months. However, as shown in Fig. 1, at day 28, stent showed sign of degradation, and at day 52 and day 90 the mechanical integrity might not be stably maintained[25].

Mg–Y–Zn alloys with different Y and Zn contents were implanted into four different tissues (liver, lesser omentum, rectus abdominis muscle and subcutaneous tissue) of Göttingen minipigs with different extents of vascularization. After 27 days, different amounts of hydrogen gas formation were observed in all tissues. After 91 days, fibrous capsules, containing some granulocytes, were observed. And in most fibrous capsules, vascularization (granulation) was observed, which implied good compatibility and signs of excellent wound healing[16].

Drynda et al. evaluated the feasibility of HF-treated Mg–Ca alloy series for stent application in a subcutaneous mouse model. The Ca content ranged from 0 to 1.0% and WE43 was used as control. After 3 months, fluoride coated pure Mg showed the largest reduction in implant area, while fluoride coated WE43 showed the least reduction in area, indicating various degradation rates. Macrophages were recognized in the implant capsule and surrounding tissues. Fibrous capsule formation was almost the same for all alloys at 6 months. Besides Mg–1.0%Ca with a less pronounced capsule formation, other alloys remained equal in

capsule formation at 3 months. Results indicated that Mg–Ca alloys had higher corrosion rates compared to WE43 and fluoride coating was a suitable way to reduce corrosion rate. However, no significant differences were observed in inflammation and capsule formation[26].

An AZ31B stent, coated by poly(lactic acid-co-trimethylene carbonate) (P(LA-TMC)) and loaded with sirolimus, was evaluated in a white rabbit aorta model. After 30 days, most of the stent remained intact, and at day 60 some struts were partially corroded, showing sign of degradation. One hundred twenty days later, most struts were completely degraded. Neointima formation and inflammatory cell infiltration were observed in all groups. However, sirolimus eluting stent had a significantly smaller neointimal area and greater lumen area compared to bare stent. A delayed endothelialization was also observed in sirolimus-eluting stent. No significant differences in inflammation and injury scores were observed in all groups[23]. This study indicated that the beneficial role sirolimus played in inhibiting neointimal formation seemed not to cause inflammation.

2.3. Clinical trials

To date, WE43 might be the only Mg alloy used for stent application in clinical trials. The AMS and Magic stent, all made of WE43, are two most frequently investigated stents in clinical trials. Several trials have been explored, not only in coronary artery diseases, but also in ischemia in limb or heart and other diseases (Table 3).

An AMS was implanted into the left pulmonary artery of a preterm baby to treat the inadvertent ligation. At second day after the implantation, serum Mg^{2+} reached maximum level at 1.7 mmol/L and decreased to normal levels within 48 h. On day 7, reperfusion of left lung was as complete as the degeneration of the affected vascular system allowed. After 33 days, the circumferential integrity of the stent was resolved and cardiac catheterization was repeated. At 5-month follow-up, the stent was completely degraded and the left lung perfusion persisted. A slight difference in size between left and right pulmonary artery was observed[29]. AMS was also used to treat critical recoarctation of aorta in a newborn. Similarly, the circumferential integrity of AMS was resolved and recatheterization was performed. A reduced diameter of aorta was observed and vessel shape was comparable as before. Then a second Mg stent, with a diameter of 4 mm and length of 15 mm, was implanted. After 3 months, ventricular septal defect closure was performed because of excess left to right shunting[30]. Reduction of lumen was observed in both studies and a repeated catheterization was required due to the degradation of AMS. In the second study, even a second Mg stent was needed. However, for newborns, the advantage of AMS over other stents is that it can adapt to the growth of the young patients.

AMS-INSIGHT clinical trial was carried out to treat below-the-knee critical limb ischemia and the control subjects were treated with percutaneous transluminal angioplasty (PTA). The safety endpoint was defined as the absence of major amputation and/or death within 30 days. The complication rates in both groups had no significant difference (5.0% vs 5.3%). The efficacy endpoint was defined as the 6-month angiographic patency rate and the control group had a significantly higher angiographic patency rate at 6-month, analyzed by two different methods. The MLD at 6-month was AMS 0.9 ± 0.7 mm vs PTA 1.4 ± 0.7 mm.

These results indicated that in long-term patency, AMS did not have efficacy over traditional PTA treatment[28]. Another clinical trial also used AMS as treatment for critical limb ischemia. After 3 months, the primary clinical patency was 89.5%. Thirteen patients had normal blood flow, 4 patients had partial stenosis and 1 patient had no blood flow[27]. Unlikely the clinical trial mentioned above, this clinical trial demonstrated the promising performance of AMS.

Erbel et al. conducted a non-randomized trial, PROGRESS-AMS clinical trial, in 63 patients with single de novo lesions. Angiography results showed a good scaffolding of the vessel with an acute lumen enlargement of 1.41 ± 0.46 mm and in-stent late loss of 1.08 ± 0.49 mm. After 4 months, a 0.83 ± 0.51 mm segment lumen loss was observed, a net gain of 0.58 ± 0.57 mm. The in-segment stenosis was 49.66% ± 16.25%. The intravascular ultrasound revealed well apposed stent struts to the vessel wall. The results showed that an immediate enlargement of vessel lumen could be achieved, the same as other metal stents. However, the results in late follow-up were not ideal[3]. Limitations, such as a small subjects pool (63 patients) and non-randomization, might have effects on the results. Another study found that in the PROGRASS-AMS clinical trial, the major contributors for restenosis were decrease of external elastic membrane volume (42%), extra-stent neointima (13%), and intrastent neointima (45%). At 4-month follow-up, the neointima was reduced by 3.6 ± 5.2 mm^3, with increase in stent cross sectional area of 0.5 ± 1.0 mm^2. The median in-stent MLD was increased from 1.87 mm to 2.17 mm, and the median angiographic late loss reduced from 0.62 mm to 0.40 mm[32].

The clinical trials above demonstrated the potential for Mg alloys in stent applications. However, the results were not ideal as expected. The radial force and the corrosion resistance are the two main directions in the future alloy development[32].

3. Bio-Adaptation between Mg Stent and Local Microenvironment

The bio-adaptation in biology is defined as the arrangements subserving specialized functions and adjustments to the needs and the mode of life of species or type[33]. In the context of implants and local microenvironment, the bio-adaptation between them means that the implants or local microenvironments change their responses or properties to the altered vicinity around them.

Arterial functional adaptations, responses to injury, and many disease processes seem to occur via similar means—a cell-mediated turnover of individual wall constituents at different rates, to different extents, and in different biomechanical environments[34]. Vessels possess the ability of continuous structural adjustment as response to local environment change and functional demands[35–38]. When stent is implanted at the stenosis site to restore overall patency of the arterial lumen and provide structural support to the vascular wall, local hemodynamics is affected due to local enlargements in artery diameter[39,40]. Meanwhile, stent deployment causes artery injury to endothelium, and overexpansion of stents may lead to intimal denudation and medial disruption. This damage and the presence of stent strut provoke the production of growth factors and cytokines, which contribute to the development of neointimal hyperplasia and restenosis[39,41]. For magnesium-based stent,

besides the altered biomechanical environment, loss of mechanical integrity[20,42,43], high magnesium ions[19], hydrogen evolution[21,44,45], and high pH[46,47] also complicate the local microenvironment.

The healing process of injured vessel is composed of inflammation, granulation formation, and remodeling. The absorbed proteins and fibrosis encapsulation may have impacts on Mg stent degradation rate and influence the local environment. The affected local microenvironment, in return, may exert effects on these healing phases.

3.1. Adaptation of stent to vessel structure and altered microenvironment

Stents must be longitudinally flexible to adapt to curved vasculature and have sufficiently low radial stiffness to prevent vascular damage[48]. Once stent is implanted, it will expand and conform to the geometry of vessel, which has been termed as stent conformity. Stent conformity is described as the flexibility of a stent in its expanded state with adaptation to the natural shape of the vessel, determining the flow rheology change within the vessel[49]. The stent design and its material are two main factors determining stent conformity[50]. Previous studies showed that open-cell design had better stent conformity than closed-cell design[51,52]. The unconnected structural elements in open-cell design contribute to longitudinal flexibility. Segmented-hoop geometry design results in stent hoop behaving fairly independently of each other. For braided geometry design, the braided wires are wrapped the entire length of the stent and not independent of each other. And stent with segmented-hoop had better adaptation to the native vessel contour[53,54]. This is probably because excessive intra-strand friction decreases the braided stent's radial and longitudinal flexibility significantly[53]. The SMART stent, composed of Nitinol, is superelastic, and this superelasticity affords Nitinol a high degree of flexibility, kink, and fatigue resistance[54]. In a study, the trackability, flexibility, and conformity of 17 commercialized coronary stents were evaluated. The varied conformity data indicated the effects of material[55].

The implanted stent changes the geometry of artery, restores the blood flow and alters the wall shear stress[40,41,56–58]. As response to the altered biomechanical environment, the biodegradation behavior of Mg stent changes. Shear stress has a strong influence on Mg alloy degradation. A low shear stress protects the surface from localized corrosion, while high shear stress leads to both uniform corrosion and localized corrosion[59]. Moreover, flow direction has a significant impact on corrosion behavior of Mg alloy. More severe pitting and erosion corrosion were observed on the back ends of MgZnCa plates, and the corrosion layer facing the flow direction was peeled off from AZ31 stent struts. The flow-induced corrosion behaviors can provide some insights for Mg stent design[60]. The biomechanical changes depend on Mg stent expansion and whether early recoil occurs or not. Little is known in the changes of restored blood flow-induced stress. The common problem in *in vivo* study is that Mg alloys are implanted into the normal animals, which cannot mimic the real scenario for altered stress in stented vessels. Therefore, atherosclerosis disease animal models should be developed in *in vivo* evaluation of Mg stent.

The stent implantation causes vascular injury, thus eliciting the wound healing response, which will be summarized in next part. In the inflammation phase, absorbed proteins also have impact on Mg stent degradation. Addition of albumin to the simulated body fluid (SBF)

can protect the oxide-protective layer of AZ91 alloy against the electrolyte attack. In a short initial time, albumin adsorption reaches peak, then less albumin is adsorbed on the AZ91 surface. However, albumin adsorption has small effect on long-term corrosion of AZ91[61]. Another study explored the absorbed albumin on the degradation behavior of Mg–Ca alloy. The results showed that the adsorption of albumin could decrease the corrosion rate and the hydrogen evolution rate. This is probably due to a mixed protective layer formed by albumin adsorption layer and $Mg(OH)_2$. Another possible reason is that negatively charged albumin molecules and OH^- may inhibit the penetration of Cl^{-1}[62]. Yamamoto and Hiromoto showed that proteins in fetal bovine serum (FBS) could retard pure Mg degradation, while amino acid promoted the Mg degradation[63].

Research showed that the location of Mg alloy in the artery also had impact on degradation. Mg wire implanted within the artery wall has a higher corrosion rate, compared to the Mg wire in contact with blood, against the artery wall. This is probably due to the formation of a calcium phosphate layer on Mg wire exposed to blood flow. For Mg wires implanted in artery, they contact with matrix and vascular cells, and the negatively charged proteoglycans in the matrix may repel the phosphate ions, thus impeding the formation of protective phosphate layer[64]. During the remodeling phase, the fibrosis encapsulation may separate the Mg stent from the blood flow. Based on this study, in the remodeling phase, contact with extracellular matrix (ECM), instead of blood flow, might promote the Mg degradation, which may be a challenge for the mechanical integrity of Mg stent.

3.2. Bio-adaptation of vessel to local microenvironment

3.2.1. Inflammation

3.2.1.1. General inflammatory responses to implanted stent: After contact with blood, the stent is spontaneously covered by a layer of proteins within seconds[65]. Thus the inflammation is initiated by the adsorption of proteins on the stent[66]. After the stent implantation, as response to the vessel injury, thrombus forms by both extrinsic and intrinsic pathways[67]. During the coagulation process, fibrin, converted from fibrinogen by thrombin, inflammatory products, released by complement system, activated platelets, and endothelial cells, form a provisional matrix on or around the implanted stent[66]. The provisional matrix provides not only structural components for the wound healing and foreign body reaction processes, but also a reservoir for mitogens, chemoattractants, cytokines, growth factors, and other bioactive agents with ability to modulate macrophage activity, proliferation, and activation of other cell populations in the inflammatory and wound healing responses[68].

The adsorbed proteins on the stent surface can modulate inflammatory cell interaction and cell adhesion[68]. Studies showed that fibrin (fibrinogen) played important roles in attracting leukocytes to implanted biomaterials[65,69] and transmitted activating signals to leukocytes[69]. The P-1 sequence, produced by the denaturation of absorbed fibrinogen, may interact with phagocyte integrin Mac-1 on simulated monocytes and neutrophils[70]. Besides the fibrinogen absorption, histamine released by mast cells in the local microenvironment is important in recruiting inflammatory cells[71]. Several cytokines are involved in modulating acute inflammation, which are summarized in Fig. 2[72]. Depending on the extent of the vascular injury, the chronic inflammation can last from minutes to days[73].

Following the acute inflammation, monocytes emigrate into the injured sites and transform into macrophages[74]. In this phase, macrophage is the most important cell. It can scavenge tissue debris and destroy any remaining neutrophils. Also the cellular and tissue phagocytosis and destruction are accomplished with the participation of macrophage. The angiogenesis, subsequent granulation tissue formation, was initiated by these processes[74,75].

3.2.1.2. Mg^{2+}: Since Mg^{2+} is an antagonist of Ca^{2+}, which is required in almost all steps in blood coagulation, low concentration of Mg^{2+} can prolong the clotting time considerably[76]. In a rat model of $FeCl_3$-induced thrombosis, high extracellular Mg^{2+}, up to 0.6 mol/L, could prevent or delay clot formation, depending on the timing of Mg^{2+} administration[77]. However, besides Ca^{2+}, studies also showed that Mg^{2+} also played a very important role in coagulation for stabilizing and regulating coagulation factor IX[78,79]. The Mg^{2+}/Ca^{2+} antagonism might reflect the influence of Mg^{2+} on inflammation. Ca deficiency has protective effect for Mg deficiency-induced inflammation[80], and abnormal Ca hemostasis that occurred during magnesium deficiency may exacerbate immune stress response at body level[81]. Another study indicated that at high Mg concentration (up to 8.0 mmol/L) *in vitro*, the leukocyte activation was diminished, probably due to the antagonist relationship between magnesium and calcium[82]. Taken together, the effect of Mg on inflammation is likely to be exerted by Mg/Ca antagonism.

3.2.1.3. H_2: During the biodegradation process, hydrogen gas (H_2) evolution is a big concern for Mg-based implants[83–86]. In human body, the evolved H_2 bubbles can be accumulated in gas cavities around the implant. The gas cavities can separate tissues and tissue layers, leading to an impeded healing process[87]. For Mg stent, H_2 evolution might be of minor importance[21,84,88], due to a thin neointimal diffusion barrier formed between stent and blood stream[21] or the removal of H_2 from the implant site by convective transport phenomena[84]. However, for local microenvironment, despite the exchange between H_2 and local tissues, H_2 could still be accumulated. Though the risk that H_2 bubbles in the blood circulating system may block the blood stream exists[89], other studies found that H_2 had beneficial effects on inflammation. At therapeutic dose, inhaled H_2 could protect against organ damages in zymosan-induced inflammation model[90]. In a mouse model of human inflammatory bowel disease, elevated levels of IL-12, TNF-α, and IL-1β in colon lesion were significantly suppressed by supplying H_2-saturated water at day 7[91]. In a spinal cord ischemic-reperfusion injury model in rabbit, 2% and 4% H_2 inhalation could effectively decrease the levels of oxidative products and pro-inflammatory cytokines and increase the activities of antioxidant enzymes[92]. Based on these studies, the protective effects of H_2 on inflammation are probably due to its antioxidant activity by selectively reducing hydroxyl radical (−OH).

3.2.1.4. $Mg(OH)_2$: In addition to Mg^{2+} and H_2, another corrosion product, magnesium hydroxide ($Mg(OH)_2$) might be involved in the inflammation process. The major source of locally released Mg^{2+} is $Mg(OH)_2$. Besides Mg^{2+} release, the dissolution of $Mg(OH)_2$ in high chloride ion environment is also accompanied by alkalosis[93]. Therefore, the effects of $Mg(OH)_2$ on inflammations may be exerted by Mg^{2+} and pH change.

3.2.1.5. pH: Previous study showed that pH was an important factor in determining the cellular picture in an inflammation area, indicating that the inflammation was associated with pH[94]. Acidic microenvironment is a common feature associated with inflammatory processes[95–101]. In the initial inflammation phase, polymorphonuclear cells predominate and the exudate is within an alkaline range (pH about 7.3–7.4). As the inflammation reaction progresses, the exudate shifts from a pH of ~7.2 to 6.8 or even lower. The acidosis is due to a glycolytic process producing lactic acid at the site of inflammation[99]. The leukocytes pump the lactic acid into the exudate, lowering the pH[100]. The polymorphonuclear cells cannot survive at such a low pH environment, then macrophages are dominated[99]. The pH value change during acute wound healing process of skin is summarized in Fig. 3[102].

The acid environment can enhance leukocytes adherence, spreading, and nitric oxide production, but suppresses phagocytosis[103]. Lower extracellular pH is also believed to induce neutrophil activation, trigger pro-inflammatory responses, delay neutrophil apoptosis, and extend its functional lifespan[101]. pH has multiple effects on TNF-α production during both transcription and translation processes in alveolar macrophage, indicating that the role of macrophage in inflammation should be modulated by extracellular pH[96]. The activation of NF-κB induced by lipopolysaccharide (LPS) was increased at extracellular pH 7.0, while attenuated at pH 6.5, compared to pH 7.4, indicating that the degree of acidosis influences inflammation[95].

In the process of Mg degradation, pH increases significantly within a short time. A small piece of corroding Mg coupon (1 cm × 1 cm × 1 cm) could increase the pH value of 250 mL neutral Hank's solution to 10 in 15 h. Theoretically, the pH value at magnesium surface is always over 10 in a neutral solution[89]. Most of the pH data during Mg alloy degradation are obtained via *in vitro* tests, because the invasive approaches to measure *in vivo* corrosion influence at least the blood flow around the implant, therefore influencing pH in the local microenvironment[104]. Though little is known about the pH range in the local vicinity, the alkalized environment may have some effects on the inflammation. The chemotaxis of polymorphonuclear leukocytes was significantly depressed at higher pH values (7.7 and 8.2), maximal at pH 7.2. However, phagocytosis of opsonized bacteria was significantly lower at pH 7.2 than that at pH 7.7[105]. Many cytokines and proteases, associated with extracellular alkalosis, are involved in the enhanced activation of inflammatory cells[106]. The p38-MAPK signaling pathway, an important pathway involved in inflammation[84,107], can be activated within 2 min at pH 8.5 or 9.5[108]. Cytosolic Ca^{2+} is involved in multiple cellular processes, and alterations of free cytosolic Ca^{2+} concentration can affect the activation of leukocyte host defense functions. And the exuberant changes in cytosolic Ca^{2+} concentration may be the cause of leukocyte hyperactivation during inflammation[103]. Studies showed that alkalosis could elevate cytosolic Ca^{2+} in macrophage[103] or increase Ca reabsorption[109].

3.2.1.6. Rare earth elements: REEs have been used to improve the corrosion resistance and mechanical strength of Mg alloys[12,110]. Most of the studies about the influence of REE on inflammation are *in vitro* tests, but little is known about *in vivo* scenario. Ce, Nd, Y and Yb at 50 μg/mL were shown to increase the expression of inflammation genes, IL-6, IL-8, and ICAM-1 in smooth muscle cell[111]. La, Pr, Nd and Y could simulate the secretion of TNF-α at 500 μmol/L and 1000 μmol/L in tumor-derived mouse macrophage cell line RAW 264.7,

while Gd could increase TNF-α expression only at 1000 μmol/L. Ce and Zr seemed to have no effects on the TNF-α expression. Compared to LPS-induced IL-1 α secretion, all the tested REE had lower expressions[110].

Some researchers explored the REE oxide *in vivo* for biomedical application. CeO_2 acts as auto-regenerative free radical scavenger and inhibits the production of pro-inflammatory iNOS protein in J774A.1 macrophage cell line[112]. In a pulmonary arterial hypertension rate model, CeO_2 attenuated monocrotaline-induced serum inflammatory markers, such as CD40 ligand, C-reactive protein, and VCAM-1[113].

3.2.1.7. In vivo inflammation scenario: As regard to implanted Mg-based stent, it is limited to investigate the effects of specific parameter on inflammation because any invasive procedure might disrupt the local microenvironment. AE21 alloy was the first investigated Mg alloy for stent application and implanted into domestic pig. No visible inflammation was found around the stented vessel and the inflammation degree was closely related to injury. The severe injury during implantation superimposed the influence of degradation on inflammation[21]. A Lekton Magic stent showed similar inflammation severity at day 28 in domestic pigs, compared to Lekton Motion stainless steel stent. Considering the injury degree was similar during implantation process, WE43 degradation products might not be attributed to the inflammation[24]. Another *in vivo* test for Lekton Magic stent in pig indicated that struts positioned within the adventitia caused inflammation, while more pronounced inflammation was observed in the most concentrated degradation products area[22]. A Biotronik Absorbed Metal Stent (AMS) was successfully implanted into re-established left lung perfusion. Five months after implantation, the patient was diagnosed with severe pneumonia and finally died from multiple organ failure. Autopsy revealed that no relevant inflammatory reaction was observed around the stent material. And the magnesium struts were mainly substituted by calcium phosphate covered by fibrotic tissue[114]. In a porcine model, AMS showed trivial inflammation at days 28, 52, and 90[25]. Based on these studies, vessel injury is one of the main sources of inflammation. The influence of degradation products on inflammation varies, probably due to Mg alloy composition difference and difference in time of animal sacrifice.

3.2.2. Granulation—Following the inflammation phase, the formation of granulation tissue is initiated by macrophage, and this process is characterized by fibroblast and SMC proliferation, ECM synthesis, and angiogenesis[75]. Therefore, the granulation formation phase is also called proliferative phase. Depending on the degree of injury, granulation tissue may be seen as early as three to five days following the implantation[73].

The activated platelets release platelet factor-4 (PF-4), platelet-derived growth factor (PDGF), and TGF-β, contributing to fibroblasts recruitment[73,115]. Moreover, numerous cytokines and growth factors secreted by macrophage and fibroblasts promote fibroblasts migration: fibroblast growth factor (FGF), insulin-like growth factor-1 (IGF-1), vascular endothelial growth factor (VEGF), IL-1, IL-2, IL-8, PDGF, TGF-α, TGF-β, and TNF-α[116]. Under normal condition, fibro-blasts and myofibroblasts are in quiescent state, with the presence of cytokines, and they are capable of migrating to the injured site and synthesizing ECM[117,118], including hyaluronan, fibronectin, proteoglycans, and type I and type III

procollagen[115]. Fibroblasts within the wound, which differ from the fibroblasts migrating from surrounding tissue, have less proliferation rate and transform to myofibroblast phenotype[116]. They contain more actin bundles, involved in wound contraction[115]. SMC also proliferated and synthesized collagen in this phase, which led to neointimal thickening[119–121]. During proliferative phase, SMC also switches its phenotype from contractile to synthetic phenotype under the stimuli of growth factors and cytokines. The SMC in synthetic phenotype produce ECM proteoglycan and collagen[121].

The growth of new blood vessels is stimulated by macrophage activity and tissue hypoxia due to disruption of blood flow at the time of injury[122]. The events are regulated by angiogenic factors, TGF-α, TGF-β, PDGF, TGF, and VEGF. As response to these angiogenic factors, endothelial cells migrate from periphery to the injured site and proliferate, forming capillary tubes[116]. Capillary sprouts invade the wound clot and a microvascular network composed of many new capillaries is formed[115].

After the formation of granulation tissue, some giant cells and the components of granulation tissue compose the foreign body reaction. The form and topography of the surface of the biomaterials determine the composition of the foreign body reaction. The foreign body reaction may persist at the tissue–implant interface for the lifetime of the implant. On the granulation tissue formation phase/proliferation phase, synthesized ECM form fibrosis or fibrous encapsulation surrounds the stent with its interfacial foreign body reaction, isolating the implant and foreign body reaction from the local tissue environment[73]. The process of fibrosis encapsulation formation is synthesized in Fig. 4[123]. Since the foreign body reaction can be categorized into inflammation, we won't discuss it in detail here.

3.2.2.1. Influence of microenvironment on granulation formation: The adhesion of WI38 human fibroblasts on type I collagen substrate is Mg^{2+}-dependent and mediated by α2β1. Moreover, Mg^{2+} supports the α2β1-mediated migration of fibroblast on type I collagen substrate. Although extracellular Ca^{2+} can reverse the adhesion of fibroblasts on collagen I, the combinations of Mg^{2+} and Ca^{2+} can enhance the migration rate by two times and the optimal migration rate is observed when Mg^{2+}/Ca^{2+} ratio is higher than 1. It is indicated that both extracellular Mg^{2+} and Ca^{2+} are involved in fibroblast migration[124]. The fluctuations of Mg^{2+}/Ca^{2+} ratio in the local wound environment are associated with cell migratory response, including fibroblast migration[125]. Calcyclin, a member of the S100 A family of calcium binding proteins, plays an important role in modulating proliferation, morphology, and cytoskeletal organization of pulmonary fibroblast[126]. Besides Mg^{2+}, pH also seems to be involved in fibroblast migration during wound healing process. In a pH range from 7.2 to 8.4, cell migration rate and DNA synthesis decrease almost in a liner manner as pH increases in experimental wounds[127].

Ca^{2+} remarkably stabilizes a recombinant 19 kDa catalytic fragment of human fibroblast collagenase, thereby influencing collagen accumulation[128]. Also the fibroblast collagenase exhibits maximal activity at neutral or slightly alkaline pH[129]. Due to antagonism with Ca^{2+}, high extracellular Mg^{2+} and highly elevated pH might be involved in collagen accumulation.

Our group previously showed that within high extracellular Mg^{2+} concentration range (10–50 mmol/L), low Mg^{2+} concentration could promote endothelial cell proliferation and migration and up-regulate the expression profiles of genes related to angiogenesis, such as FGF1, VEGFA and NOS3[130]. Another study also indicated that within relatively low Mg^{2+} concentration range (2–10 mmol/L), high concentration of Mg^{2+} stimulated endothelial cell proliferation, enhanced mitogenic response to angiogenic factors and enhanced the synthesis of nitric oxide[131]. Mg^{2+} also promoted endothelial cell spreading on gelatin, type IV collagen and vitronectin at 10 mmol/L. Mg^{2+} induced both chemokinetic and chemotactic migration peaking at 0.1 and 10 mmol/L[132]. These studies suggested that the local microenvironment, such as Mg^{2+} and high pH, had effects on fibroblast migration, collagen synthesis and angiogenesis.

3.2.2.2. In vivo granulation formation: Early in 1930s, researchers found the granulation tissue formation and contained foreign body giant cells with little black metallic particles as foreign body inclusions around corroding Mg[86]. In a mouse tail model, pure magnesium wires were implanted and granulation tissues were observed at 4 weeks, overlapping with fibrous capsules partly[133]. In one study, magnesium alloy RS66 was implanted into three different sites of rabbits, cancellous bone of medial femur condyle, lumbar musculature and subcutaneous tissue. Only a thin layer of granulation tissue was observed around bone–implant interface both at 4 and 8 weeks[134]. Open porous scaffolds made of AZ91D were implanted into the right knee. From 3 months to 6 months, the space left by the degrading implant was filled up by granulation tissue[45]. In a previous study, Janning et al.[93] implanted $Mg(OH)_2$ cylinder into knees joints of rabbit and knee drilled holes were used as control group. After two weeks, for control group, most parts of the drilled holes were filled with granulation tissue. After 4 and 6 weeks, this granulation tissue had been replaced by woven bone, while for $Mg(OH)_2$ implanted bone no granulation tissue was observed. But the cylinder dissolved at the same pace of bone ingrowth[93]. In another study conducted by Willbold et al.[135], Mg-REE alloys were also implanted into the knee joint of rabbits and the control groups were drill holes. Similar results were observed. Granulation tissues were formed in drilled holes after 4 weeks[135]. An Mg–Zn–Mn alloy rod was implanted into the femora of rats. No granulation tissue was observed both at 6 and 26 weeks around bone–implant interface[136].

The granulation tissue acts as the bridge between two sutures. Depending on the degree of injury or defect created by implantation procedure, two wound healing responses occur. Wound healing by primary intension involves the closure of a clean, non-infected surgical incision with sutures approximating the wound edges. A small amount of granulation tissue forms in this response and this type of healing relies on the rejoining of the connective tissue matrix. In contrast, healing by secondary intension involves the closure of a large open defect. The regenerated parenchymal cells cannot completely reconstitute the original architecture. Significant granulation tissues are needed, resulting in larger areas of fibrosis or scar formation[73,137]. For Mg stent application, the healing response may be the primary intension. As Mg stent degrades, the space left by Mg stent will be replaced by granulation tissue, and during wound remodeling phase endothelial cells must be over the granulation tissue[138]. For stent application, researchers focus on inflammation and neointimal

formation in animal tests. Due to limited access to histological analysis, granulation formation analysis seems impossible in clinical trial. Therefore, to date, few researchers have reported the granulation formation in Mg stent application.

3.2.3. Remodeling—The remodeling phase involves a balance between synthesis and degradation and reorganization of ECM deposited in the wound[139]. It is responsible for the development of endothelium and final scar formation. ECM synthesis in proliferative and remodeling phases is initiated contemporarily with granulation formation[115]. The deposited ECM composition changes over the wound healing process. Initially it is composed mainly of fibrin and fibronectin, resulting from hemostasis and macrophage. In the granulation tissue, the amount of collagen III increases, while after maturation the collagen III is mainly replaced by collagen I[115,140]. Scar may regain 80% of original strength in the long term, but the original strength can never be achieved[115,139].

The remodeling events are tightly regulated by matrix metalloproteinases (MMPs) and tissue inhibitor of metalloproteinases (TIMPs)[141]. Sources of MMPs are neutrophils, macrophages, and fibroblasts in the wound. MMPs are responsible for the degradation of collagen. The activity of TIMPs increases gradually, thereby promoting the accumulation of new matrix. During this process, new collagen is synthesized and old collagen is lysed[74,115]. PDGF and TGF-β are also involved in the ECM regulation[142].

Mg^{2+} seems to decrease the MMP-2 production induced by homocysteine in vascular smooth muscle cell in a low concentration range (0.5–3 mmol/L). Also magnesium-deficient diet (50 ± 5 ppm) for 42 days could induce a thinner aortic wall, compared to the control diet (1700 ± 100). The MMP-2 and MMP-9 in magnesium-deficient mice were present in active and inactive forms, respectively[143]. MMP has the optimal activity at pH 7.2. Elevated pH (7.4) and decreased pH (down to 6.4) impair the activity of MMP both in bovine articular chondrocytes and nucleus pulpous cells[144]. Another study showed that the gelatinolytic activity for MMP-9 was optimal at pH 7.5, and 50%–80% of full activity was retained in acidic environment (pH 5.5–6.0). Even at lower pH (2.3), the zymogen of MMP-9 can also be activated up to 85% of full activity. Moreover, high concentration of Ca^{2+} enhanced the degradation of acid-soluble and acid-insoluble collagen I by MMP-9[145]. These studies indicate that the high extracellular pH and Mg^{2+} in the local microenvironment can influence the remodeling phase.

Blood vessels can enlarge to adapt to the increased blood flow. The vessels have a compensation mechanism, enlarging the radial diameter, to adapt to the progressive development of atherosclerotic plaques. Even though most atherosclerotic segments exhibit some compensatory enlargement, it is still inadequate to completely preserve the lumen size. Moreover, some vessels may shrink at the lesion site, namely inward remodeling[146]. Although implantation of a stent limits artery shrinkage, it may not limit remodeling, because the arterial wall may be squeezed through the stent strut interstices from outside, leading to negative remodeling[120]. As regard to Mg stent, this complication may not happen since ideally degradation of Mg stent matches with granulation formation and later remodeling. In addition, the mechanical support provided by Mg stent is replaced by remodeled ECM gradually.

The *in vivo* vascular remodeling of available Mg stent is not as ideal as expected. In the first Mg-based stent application in domestic pigs, 40% loss of lumen diameter between day 10 and day 35 was observed because of neointima formation. A 25% re-enlargement between day 35 and day 56 was also observed, due to vascular modeling[21]. In a study, Lekton Magic stents were implanted into 33 minipigs, and Lekton Motion made of 316 L stainless steel was used as control. After 4 weeks, Mg group had higher lumen diameter than control group (1.49 mm vs 1.34 mm). After 2 months, the lumen diameter of control group remained nearly unchanged, while Mg group revealed significant vascular remodeling: lumen diameter increased from 1.49 mm at week 4 to 1.68 mm at week 12[22]. This indicates that Mg stent inhibits, or at least does not promote, neointimal formation in the early phase. Then in later remodeling phase, the Mg stent enlarges the vessel due to degradation. In a similar study, Waksman et al. implanted Lekton Magic stent into domestic pigs and minipigs, and the control was Lekton Motion stent. Compared to the control group, the neointimal area was significantly less in Mg alloy stent segments at 28 days (2.44 ± 0.88 mm^2 vs 5.03 ± 1.5 mm^2) and at 3 months (1.16 ± 0.19 mm^2 vs 1.72 ± 0.68 mm^2). Both groups showed significant vascular remodeling from 28 days to 3 months[24].

Based on the animal studies, Mg-based stent has the potential in preventing artery shrinkage. And in later remodeling phase, due to biodegradation, the space left is filled with granulation tissue at first, finally replaced by fibrosis. However, the reduction of neointima does not mean enlarged diameter. Compared to unstented vessel, the diameter of stented vessel is still narrow[21,24]. Moreover, the greatest concentrated Mg degradation products elicit pronounced inflammation[22].

The main functions of Mg stent are to provide time and space for injury healing. Previous study suggested that restenosis usually occurred within the first 6 months after stenting, with minimal changes occurring thereafter[147]. Other researchers indicated that a complete degradation was expected after the remodeling phase, usually occurring at 90–120 days. Due to insufficient *in vivo* data available especially for the vessel wall mechanical properties during healing process, though it is still arguable whether full mechanical support is necessary within the first 4 months, it would be a safety design parameter[5]. The ideal relationship between mechanical integrity and stent degradation is summarized in Fig. 5[148].

These complications in vessel responses to local microenvironment during inflammation, granulation formation, and remodeling phases require better alloy development and stent design. In addition, the stent implantation procedure should be improved to reduce the vascular injury. We will discuss the future directions for Mg stent research and other perspectives in the next part.

4. Future Research Perspectives

Stenting has been used to treat narrowed or blocked coronary vessel for a very long time[149]. The interaction of a stent with its surrounding tissues as well as the whole biological system determines the success of the stent material. No matter it is Mg-based stent material or traditional stent materials including titanium, cobalt-chromium alloy, and stainless steel, all those materials could change the mechanical, chemical and biological

microenvironments after implantation. Although, a few published clinical applications of Mg-based stent material have shown some promising results[3,4,27,150], to better understand the exact mechanism about how local blood tissue and whole system adapt to the implanted stent will no doubt further improve the safety and effectiveness of stent application.

From a biomechanical perspective, maintaining sufficient radial strength before the vascular healing is inevitable for a stent material. One question with respect to the mechanical properties of a stent is to find the optimal supporting force for different part of blood vessels. How much force is needed to support the blood vessel so that enough lumen size can be maintained and the supporting strength won't cause severe tissue stress? Under the same design criterion, materials with relative high yield strength and ultimate strength could provide higher mechanical support. The yield strength and ultimate strength of most Mg-based materials are among 100 to 400 MPa, which is enough for vascular stent application. The elongation of the materials should be higher than 15% to satisfy the stent expansion requirement. Besides, tailoring the design and size of a stent based on the individual vessel structure may further improve the chance of success. Other potential problems of metallic stent such as impairment of vessel geometry and alteration of hemodynamics caused by the presence of a stent should also be considered. It was known that the mechanical properties of an Mg-based stent will decrease with the progress of degradation. The degradation process within the initial 4 months should be slow enough so that the mechanical properties of the stent will not be compromised. After the vascular vessel regains enough strength, a fast degradation rate is preferred to remove the unnecessary presence of the stent. Therefore, how to match the degradation rate for a material with the local tissues healing speed is a fundamental question for degradable stent material. Earlier degraded stent could lead to recoil or collapse of the stent resulting in vascular occlusion, while late full degradation may cause chronic inflammation and immune responses. The degradation rate of Mg-based stent material is decided by the composition of material, material manufacture process, stent design, and physiological microenvironment of the blood vessel. Controlling some of those parameters to optimize the corrosion behavior of Mg material is still a very attractive research direction to improve the bio-adaptation between local tissue and the stent material.

Another essential question about Mg material for vascular stent application is how to reduce the biological stress caused by a stent. Due to the fact that it is impossible to avoid all the negative cellular and tissue responses to a non-biological object, identifying the major factors could provide new directions to improve the bio-adaptation. It has been known for a long time that toxicity from stent degradation products could lead to poor bio-adaptability of local blood vessel to the stent material. The Mg material itself, release of alloying element ions, particulate products, and presence of hydrogen gas bubble, could, to different extents, affect the local cell and tissue adaptation. Poor endothelialization and over-proliferation of smooth muscle cell around the stent are the direct maladaptation results. As a non-biological substance, Mg-based stent non-specifically adsorbs biomacromolecules after implantation. On one hand, this non-specific adsorption is beneficial for cell attachment and proliferation. On the other hand, it could contribute to initiation of platelets, inflammatory reaction, or foreign body reaction. How to prevent those biomolecules that initiate inflammatory responses or immune responses might be a way to further improve the bio-adaptation between a stent and the blood vessel. Drug eluting stents, such as paclitaxel, have shown

better late stage performance compared with bare Mg-based stent[4]. Other than those anti-proliferation drugs, signaling molecules (protein and RNA), gene and even human cells could potentially be used to improve the bio-adaptation. In addition, the signaling pathways and crosstalk between human tissues and biomaterial, not only Mg-based materials, are still elusive. We believe that solving those questions will help to further improve the bio-adaptation between Mg-based stent material and host body.

References

1. Zhao N, Watson N, Xu Z, Chen Y, Waterman J, Sankar J, Zhu D. PLoS ONE. 2014; 9:e98674. [PubMed: 24921251]
2. Gong H, Wang K, Strich R, Zhou JG. J Biomed Mater Res Part B Appl Biomater. 2015; 103:1632–1640. [PubMed: 25581552]
3. Erbel R, Di Mario C, Bartunek J, Bonnier J, de Bruyne B, Eberli FR, Erne P, Haude M, Heublein B, Horrigan M. Lancet. 2007; 369:1869–1875. [PubMed: 17544767]
4. Haude M, Erbel R, Erne P, Verheye S, Degen H, Böse D, Vermeersch P, Wijnbergen I, Weissman N, Prati F. Lancet. 2013; 381:836–844. [PubMed: 23332165]
5. Zheng Y, Gu X, Witte F. Mater Sci Eng R. 2014; 77:1–34.
6. Drynda A, Hassel T, Hoehn R, Perz A, Bach FW, Peuster M. J Biomed Mater Res A. 2010; 93:763–775. [PubMed: 19653306]
7. Mao L, Yuan G, Niu J, Zong Y, Ding W. Mater Sci Eng C. 2013; 33:242–250.
8. Zhou W, Zheng Y, Leeflang M, Zhou J. Acta Biomater. 2013; 9:8488–8498. [PubMed: 23385218]
9. Guo M, Cao L, Lu P, Liu Y, Xu X. J Mater Sci Mater Med. 2011; 22:1735–1740. [PubMed: 21630093]
10. Bornapour M, Muja N, Shum-Tim D, Cerruti M, Pekguleryuz M. Acta Biomater. 2013; 9:5319–5330. [PubMed: 22871640]
11. Mao L, Shen L, Niu J, Zhang J, Ding W, Wu Y, Fan R, Yuan G. Nanoscale. 2013; 5:9517–9522. [PubMed: 23989064]
12. Pérez P, Onofre E, Cabeza S, Llorente I, Del Valle J, García-Alonso M, Adeva P, Escudero M. Corros Sci. 2013; 69:226–235.
13. Gu X, Zhou W, Zheng Y, Cheng Y, Wei S, Zhong S, Xi T, Chen L. Acta Biomater. 2010; 6:4605–4613. [PubMed: 20656074]
14. Wiebe J, Nef HM, Hamm CW. J Am Coll Cardiol. 2014; 64:2541–2551. [PubMed: 25500240]
15. Hänzi AC, Sologubenko AS, Uggowitzer PJ. Mater Sci Forum. 2009; 618:75–82.
16. Hänzi AC, Gerber I, Schinhammer M, Löffler JF, Uggowitzer PJ. Acta Biomater. 2010; 6:1824–1833. [PubMed: 19815099]
17. Loos A, Rohde R, Haverich A, Barlach S. Macromol Symp. 2007; 253:103–108.
18. Lu P, Cao L, Liu Y, Xu X, Wu X. J Biomed Mater Res Part B Appl Biomater. 2011; 96:101–109. [PubMed: 21053265]
19. Lu P, Fan H, Liu Y, Cao L, Wu X, Xu X. Colloids Surf B Biointerfaces. 2011; 83:23–28. [PubMed: 21087842]
20. Li N, Zheng Y. J Mater Sci Technol. 2013; 29:489–502.
21. Heublein B, Rohde R, Kaese V, Niemeyer M, Hartung W, Haverich A. Heart. 2003; 89:651–656. [PubMed: 12748224]
22. Di Mario C, Griffiths H, Goktekin O, Peeters N, Verbist J, Bosiers M, Deloose K, Heublein B, Rohde R, Kasese V. J Interv Cardiol. 2004; 17:391–395. [PubMed: 15546291]
23. Li H, Zhong H, Xu K, Yang K, Liu J, Zhang B, Zheng F, Xia Y, Tan L, Hong D. J Endovasc Ther. 2011; 18:407–415. [PubMed: 21679083]
24. Waksman R, Pakala R, Kuchulakanti PK, Baffour R, Hellinga D, Seabron R, Tio FO, Wittchow E, Hartwig S, Harder C. Catheter Cardiovasc Interv. 2006; 68:607–617. [PubMed: 16969879]

25. Slottow TLP, Pakala R, Okabe T, Hellinga D, Lovec RJ, Tio FO, Bui AB, Waksman R. Cardiovasc Revasculariz Med. 2008; 9:248–254.
26. Drynda A, Seibt J, Hassel T, Bach FW, Peuster M. J Biomed Mater Res A. 2013; 101:33–43. [PubMed: 22767427]
27. Peeters P, Bosiers M, Verbist J, Deloose K, Heublein B. J Endovasc Ther. 2005; 12:1–5. [PubMed: 15683259]
28. Bosiers M. Investigators AI. Cardiovasc Intervent Radiol. 2009; 32:424–435. [PubMed: 19093148]
29. Zartner P, Cesnjevar R, Singer H, Weyand M. Catheter Cardiovasc Interv. 2005; 66:590–594. [PubMed: 16206223]
30. Schranz D, Zartner P, Michel-Behnke I, Akintürk H. Catheter Cardiovasc Interv. 2006; 67:671–673. [PubMed: 16575923]
31. McMahon CJ, Oslizlok P, Walsh KP. Catheter Cardiovasc Interv. 2007; 69:735–738. [PubMed: 17330269]
32. Waksman R, Erbel R, Di Mario C, Bartunek J, de Bruyne B, Eberli FR, Erne P, Haude M, Horrigan M, Ilsley C. JACC Cardiovasc Interv. 2009; 2:312–320. [PubMed: 19463443]
33. Corning PA. J Bioecon. 2000; 2:41–86.
34. Ogden, RW.; Holzapfel, GA. Mechanics of Biological Tissue. Springer; 2006.
35. Pries A, Reglin B, Secomb T. Am J Physiol Heart Circ Physiol. 2001; 281:H1015–H1025. [PubMed: 11514266]
36. Pries A, Secomb T, Gaehtgens P. Am J Physiol Heart Circ Physiol. 1998; 275:H349–H360.
37. Pries AR, Reglin B, Secomb TW. Hypertension. 2005; 46:725–731. [PubMed: 16172421]
38. Pries AR, Secomb TW, Gaehtgens P. Hypertension. 1999; 33:153–161. [PubMed: 9931096]
39. Seo T, Schachter LG, Barakat AI. Ann Biomed Eng. 2005; 33:444–456. [PubMed: 15909650]
40. Warltier DC, Kersten JR, Pagel PS. Biomed Eng Online. 2006; 5:40. [PubMed: 16780592]
41. Gijsen FJ, Migliavacca F, Schievano S, Socci L, Petrini L, Thury A, Wentzel JJ, van der Steen A, Serruys P, Dubini G. Biomed Eng Online. 2008; 7:23. [PubMed: 18684321]
42. Grogan J, O'Brien B, Leen S, McHugh P. Acta Biomater. 2011; 7:3523–3533. [PubMed: 21664498]
43. Wang H, Guan S, Wang X, Ren C, Wang L. Acta Biomater. 2010; 6:1743–1748. [PubMed: 20004746]
44. Kuhlmann J, Bartsch I, Willbold E, Schuchardt S, Holz O, Hort N, Höche D, Heineman WR, Witte F. Acta Biomater. 2013; 9:8714–8721. [PubMed: 23069319]
45. Witte F, Ulrich H, Rudert M, Willbold E. J Biomed Mater Res A. 2007; 81:748–756. [PubMed: 17390368]
46. Witte F, Kaese V, Haferkamp H, Switzer E, Meyer-Lindenberg A, Wirth CJ, Windhagen H. Biomaterials. 2005; 26:3557–3563. [PubMed: 15621246]
47. Zeng R, Dietzel W, Witte F, Hort N, Blawert C. Adv Eng Mater. 2008; 10:B3–B14.
48. De Bock S, Iannaccone F, De Santis G, De Beule M, Mortier P, Verhegghe B, Segers P. J Biomech. 2012; 45:1353–1359. [PubMed: 22483228]
49. Gomez-Lara J, Garcia-Garcia HM, Onuma Y, Garg S, Regar E, De Bruyne B, Windecker S, McClean D, Thuesen L, Dudek D. JACC Cardiovasc Interv. 2010; 3:1190–1198. [PubMed: 21087756]
50. e Silva MV, Costa JR, Abizaid A, Staico R, Taiguara D, Borghi TC, Costa R, Chamié D, Sousa AG, Sousa JE. Rev Bras Cardiol Invas Eng Vers. 2013; 21:332–337.
51. Conti M, Van Loo D, Auricchio F, De Beule M, De Santis G, Verhegghe B, Pirrelli S, Odero A. J Endovasc Ther. 2011; 18:397–406. [PubMed: 21679082]
52. Sangiorgi G, Melzi G, Agostoni P, Cola C, Clementi F, Romitelli P, Virmani R, Colombo A. Ann Ist Super Sanita. 2006; 43:89–100. [PubMed: 17536159]
53. Ma D, Dargush GF, Natarajan SK, Levy EI, Siddiqui AH, Meng H. J Biomech. 2012; 45:2256–2263. [PubMed: 22818662]
54. Phatouros CC, Higashida RT, Malek AM, Meyers PM, Lempert TE, Dowd CF, Halbach VV. AJNR Am J Neuroradiol. 2000; 21:732–738. [PubMed: 10782787]

55. Rieu R, Barragan P, Garitey V, Roquebert PO, Fuseri J, Commeau P, Sainsous J. Catheter Cardiovasc Interv. 2003; 59:496–503. [PubMed: 12891615]
56. Holzapfel GA, Stadler M, Gasser TC. J Biomech Eng. 2005; 127:166–180. [PubMed: 15868799]
57. LaDisa JF, Hettrick DA, Olson LE, Guler I, Gross ER, Kress TT, Kersten JR, Warltier DC, Pagel PS. J Appl Physiol. 2002; 93:1939–1946. [PubMed: 12391052]
58. LaDisa JF, Olson LE, Hettrick DA, Warltier DC, Kersten JR, Pagel PS. Biomed Eng Online. 2005; 4:59. [PubMed: 16250918]
59. Lévesque J, Hermawan H, Dubé D, Mantovani D. Acta Biomater. 2008; 4:284–295. [PubMed: 18033745]
60. Wang J, Giridharan V, Shanov V, Xu Z, Collins B, White L, Jang Y, Sankar J, Huang N, Yun Y. Acta Biomater. 2014; 10:5213–5223. [PubMed: 25200844]
61. Liu C, Xin Y, Tian X, Chu PK. J Mater Res. 2007; 22:1806–1814.
62. Liu C, Wang Y, Zeng R, Zhang X, Huang W, Chu P. Corros Sci. 2010; 52:3341–3347.
63. Yamamoto A, Hiromoto S. Mater Sci Eng C. 2009; 29:1559–1568.
64. Pierson D, Edick J, Tauscher A, Pokorney E, Bowen P, Gelbaugh J, Stinson J, Getty H, Lee CH, Drelich J. J Biomed Mater Res Part B Appl Biomater. 2012; 100:58–67. [PubMed: 21905215]
65. Tang L, Eaton JW. J Exp Med. 1993; 178:2147–2156. [PubMed: 8245787]
66. Luttikhuizen DT, Harmsen MC, Luyn MJV. Tissue Eng. 2006; 12:1955–1970. [PubMed: 16889525]
67. Dahlbäck B. Lancet. 2000; 355:1627–1632. [PubMed: 10821379]
68. Anderson JM, Rodriguez A, Chang DT. Semin Immunol. 2008; 20:86–100. [PubMed: 18162407]
69. Smiley ST, King JA, Hancock WW. J Immunol. 2001; 167:2887–2894. [PubMed: 11509636]
70. Mosesson M. J Thromb Haemost. 2005; 3:1894–1904. [PubMed: 16102057]
71. Zdolsek J, Eaton JW, Tang L. J Transl Med. 2007; 5:31–36. [PubMed: 17603911]
72. Feghali CA, Wright TM. Front Biosci. 1997; 2:d12–d26. [PubMed: 9159205]
73. Anderson JM. Ann Rev Mater Res. 2001; 31:81–110.
74. Li J, Chen J, Kirsner R. Clin Dermatol. 2007; 25:9–18. [PubMed: 17276196]
75. Babensee JE, Anderson JM, McIntire LV, Mikos AG. Adv Drug Deliv Rev. 1998; 33:111–139. [PubMed: 10837656]
76. Huntsman RG, Hurn BAL, Lehmann H. J Clin Pathol. 1960; 13:99–101. [PubMed: 14405485]
77. Mussoni L, Sironi L, Tedeschi L, Calvio AM, Colli S, Tremoli E. Thromb Haemost. 2001; 86:1292–1295. [PubMed: 11816720]
78. Sekiya F, Yamashita T, Atoda H, Komiyama Y, Morita T. J Biol Chem. 1995; 270:14325–14331. [PubMed: 7782291]
79. Sekiya F, Yoshida M, Yamashita T, Morita T. J Biol Chem. 1996; 271:8541–8544. [PubMed: 8621478]
80. Gueux E, Rock E, Mazur A, Rayssiguier Y. Eur J Nutr. 2002; 41:197–202. [PubMed: 12395213]
81. Malpuech-Brugère C, Rock E, Astier C, Nowacki W, Mazur A, Rayssiguier Y. Life Sci. 1998; 63:1815–1822. [PubMed: 9820125]
82. Bussiere F, Mazur A, Fauquert J, Labbe A, Rayssiguier Y, Tridon A. Magnes Res. 2002; 15:43–48. [PubMed: 12030423]
83. Chen Y, Xu Z, Smith C, Sankar J. Acta Biomater. 2014; 10:4561–4573. [PubMed: 25034646]
84. Persaud-Sharma D, McGoron A. J Biomim Biomater Biomed Eng. 2012; 12:25–39.
85. Poinern GEJ, Brundavanam S, Fawcett D. Am J Biomed Eng. 2012; 2:218–240.
86. Witte F. Acta Biomater. 2010; 6:1680–1692. [PubMed: 20172057]
87. Meyer-Lindenberg A, Windhugen H, Witte F. Google Patents. 2002
88. Zberg B, Uggowitzer PJ, Löffler JF. Nat Mater. 2009; 8:887–891. [PubMed: 19783982]
89. Song G. Corros Sci. 2007; 49:1696–1701.
90. Xie K, Yu Y, Zhang Z, Liu W, Pei Y, Xiong L, Hou L, Wang G. Shock. 2010; 34:495–501. [PubMed: 20351628]

91. Kajiya M, Silva MJ, Sato K, Ouhara K, Kawai T. Biochem Biophys Res Commun. 2009; 386:11–15. [PubMed: 19486890]
92. Huang Y, Xie K, Li J, Xu N, Gong G, Wang G, Yu Y, Dong H, Xiong L. Brain Res. 2011; 1378:125–136. [PubMed: 21195696]
93. Janning C, Willbold E, Vogt C, Nellesen J, Meyer-Lindenberg A, Windhagen H, Thorey F, Witte F. Acta Biomater. 2010; 6:1861–1868. [PubMed: 20035905]
94. Menkin V. Am J Pathol. 1934; 10:193–210. [PubMed: 19970136]
95. de Nadai TR, de Nadai MN, Albuquerque AAS, de Carvalho MTM, Celotto AC, Evora PRB. Int J Inflam. 2013; 2013:601424. [PubMed: 23841017]
96. Heming TA, Dave SK, Tuazon DM, Chopra AK, Peterson JW, Bidani A. Clin Sci (Lond). 2001; 101:267–274. [PubMed: 11524044]
97. Kato Y, Ozawa S, Miyamoto C, Maehata Y, Suzuki A, Maeda T, Baba Y. Cancer Cell Int. 2013; 13:89. [PubMed: 24004445]
98. King B, Wildman S, Ziganshina L, Pintor J, Burnstock G. Br J Pharmacol. 1997; 121:1445–1453. [PubMed: 9257926]
99. Menkin V. Br Med J. 1960; 1:1521–1528. [PubMed: 20788900]
100. Steen KH, Steen AE, Reeh PW. J Neurosci. 1995; 15:3982–3989. [PubMed: 7751959]
101. Trevani AS, Andonegui G, Giordano M, López DH, Gamberale R, Minucci F, Geffner JR. J Immunol. 1999; 162:4849–4857. [PubMed: 10202029]
102. Schneider LA, Korber A, Grabbe S, Dissemond J. Arch Dermatol Res. 2007; 298:413–420. [PubMed: 17091276]
103. Heming TA, Bulayeva NN, Bidani A. Clin Sci. 2003; 105:21–28. [PubMed: 12593669]
104. Witte F, Fischer J, Nellesen J, Crostack HA, Kaese V, Pisch A, Beckmann F, Windhagen H. Biomaterials. 2006; 27:1013–1018. [PubMed: 16122786]
105. Leblebicioglu B, Lim JS, Cario AC, Beck FM, Walters JD. J Periodontol. 1996; 67:472–477. [PubMed: 8724704]
106. Corbel M, Belleguic C, Boichot E, Lagente V. Cell Biol Toxicol. 2002; 18:51–61. [PubMed: 11991086]
107. Han J, Jiang Y, Li Z, Kravchenko V, Ulevitch R. Nature. 1997; 386:296–299. [PubMed: 9069290]
108. Stathopoulou K, Gaitanaki C, Beis I. J Exp Biol. 2006; 209:1344–1354. [PubMed: 16547305]
109. Rouse D, Suki WN. Kidney Int. 1990; 38:700–708. [PubMed: 2232507]
110. Feyerabend F, Fischer J, Holtz J, Witte F, Willumeit R, Drücker H, Vogt C, Hort N. Acta Biomater. 2010; 6:1834–1842. [PubMed: 19800429]
111. Drynda A, Deinet N, Braun N, Peuster M. J Biomed Mater Res A. 2009; 91:360–369. [PubMed: 18980223]
112. Hirst SM, Karakoti AS, Tyler RD, Sriranganathan N, Seal S, Reilly CM. Small. 2009; 5:2848–2856. [PubMed: 19802857]
113. Kolli MB, Manne ND, Para R, Nalabotu SK, Nandyala G, Shokuhfar T, He K, Hamlekhan A, Ma JY, Wehner PS. Biomaterials. 2014; 35:9951–9962. [PubMed: 25224369]
114. Zartner P, Buettner M, Singer H, Sigler M. Catheter Cardiovasc Interv. 2007; 69:443–446. [PubMed: 17295281]
115. Velnar T, Bailey T, Smrkolj V. J Int Med Res. 2009; 37:1528–1542. [PubMed: 19930861]
116. Teller P, White TK. Perioper Nurs Clin. 2011; 6:159–170.
117. Maltseva O, Folger P, Zekaria D, Petridou S, Masur SK. Invest Ophthalmol Vis Sci. 2001; 42:2490–2495. [PubMed: 11581188]
118. Meran S, Thomas D, Stephens P, Martin J, Bowen T, Phillips A, Steadman R. J Biol Chem. 2007; 282:25687–25697. [PubMed: 17611197]
119. Costa MA, Simon DI. Circulation. 2005; 111:2257–2273. [PubMed: 15867193]
120. Edelman ER, Rogers C. Am J Cardiol. 1998; 81:4E–6E.
121. Forrester JS, Fishbein M, Helfant R, Fagin J. J Am Coll Cardiol. 1991; 17:758–769. [PubMed: 1993798]
122. Flanagan M. J Wound Care. 2000; 9:299–300. [PubMed: 11933346]

123. Ratner BD. J Control Release. 2002; 78:211–218. [PubMed: 11772462]
124. Grzesiak JJ, Davis GE, Kirchhofer D, Pierschbacher MD. J Cell Biol. 1992; 117:1109–1117. [PubMed: 1374416]
125. Grzesiak JJ, Pierschbacher MD. J Clin Invest. 1995; 95:227–233. [PubMed: 7814620]
126. Breen EC, Tang K. J Cell Biochem. 2003; 88:848–854. [PubMed: 12577318]
127. Lengheden A, Jansson L. Eur J Oral Sci. 1995; 103:148–155. [PubMed: 7634130]
128. Lowry CL, McGeehan G, Le Vine H. Proteins Struct Funct Genet. 1992; 12:42–48. [PubMed: 1313176]
129. Birkedal-Hansen H, Cobb CM, Taylor RE, Fullmer H. J Biol Chem. 1976; 251:3162–3168. [PubMed: 57961]
130. Zhao N, Zhu D. Metallomics. 2015; 7:113–123.
131. Maier JA, Bernardini D, Rayssiguier Y, Mazur A. Biochim Biophys Acta. 2004; 1689:6–12. [PubMed: 15158908]
132. Lapidos KA, Woodhouse EC, Kohn EC, Masiero L. Angiogenesis. 2001; 4:21–28. [PubMed: 11824374]
133. Badar M, Lünsdorf H, Evertz F, Rahim MI, Glasmacher B, Hauser H, Mueller PP. Acta Biomater. 2013; 9:7580–7589. [PubMed: 23518475]
134. Willbold E, Kalla K, Bartsch I, Bobe K, Brauneis M, Remennik S, Shechtman D, Nellesen J, Tillmann W, Vogt C. Acta Biomater. 2013; 9:8509–8517. [PubMed: 23416472]
135. Willbold E, Gu X, Albert D, Kalla K, Bobe K, Brauneis M, Janning C, Nellesen J, Czayka W, Tillmann W. Acta Biomater. 2015; 11:554–562. [PubMed: 25278442]
136. Zhang E, Xu L, Yu G, Pan F, Yang K. J Biomed Mater Res A. 2009; 90:882–893. [PubMed: 18618719]
137. Drew AF, Liu H, Davidson JM, Daugherty CC, Degen JL. Blood. 2001; 97:3691–3698. [PubMed: 11389004]
138. Grillo HC. Ann Thorac Surg. 2002; 73:1995–2004. [PubMed: 12078821]
139. Young A, McNaught CE. Surgery (Oxford). 2011; 29:475–479.
140. Witte MB, Barbul A. Surg Clin North Am. 1997; 77:509–528. [PubMed: 9194878]
141. Madlener M, Parks WC, Werner S. Exp Cell Res. 1998; 242:201–210. [PubMed: 9665817]
142. Schultz GS, Wysocki A. Wound Repair Regen. 2009; 17:153–162. [PubMed: 19320882]
143. Pages N, Gogly B, Godeau G, Igondjo-Tchen S, Maurois P, Durlach J, Bac P. Magnes Res. 2003; 16:43–48. [PubMed: 12735482]
144. Razaq S, Wilkins RJ, Urban JP. Eur Spine J. 2003; 12:341–349. [PubMed: 12883962]
145. Okada Y, Naka K, Kawamura K, Matsumoto T, Nakanishi I, Fujimoto N, Sato H, Seiki M. Lab Invest. 1995; 72:311–322. [PubMed: 7898050]
146. Ward MR, Pasterkamp G, Yeung AC, Borst C. Circulation. 2000; 102:1186–1191. [PubMed: 10973850]
147. Schömig A, Kastrati A, Mudra H, Blasini R, Schühlen H, Klauss V, Richardt G, Neumann FJ. Circulation. 1994; 90:2716–2724. [PubMed: 7994813]
148. Hermawan H, Dubé D, Mantovani D. Acta Biomater. 2010; 6:1693–1697. [PubMed: 19815097]
149. Stefanini GG, Holmes DR Jr. N Engl J Med. 2013; 368:254–265. [PubMed: 23323902]
150. Haude M, Erbel R, Erne P, Verheye S, Vermeersch P, Degen H, Boese D, Waksman R, Weissman N, Prati F. J Am Coll Cardiol. 2013; 62:B13.

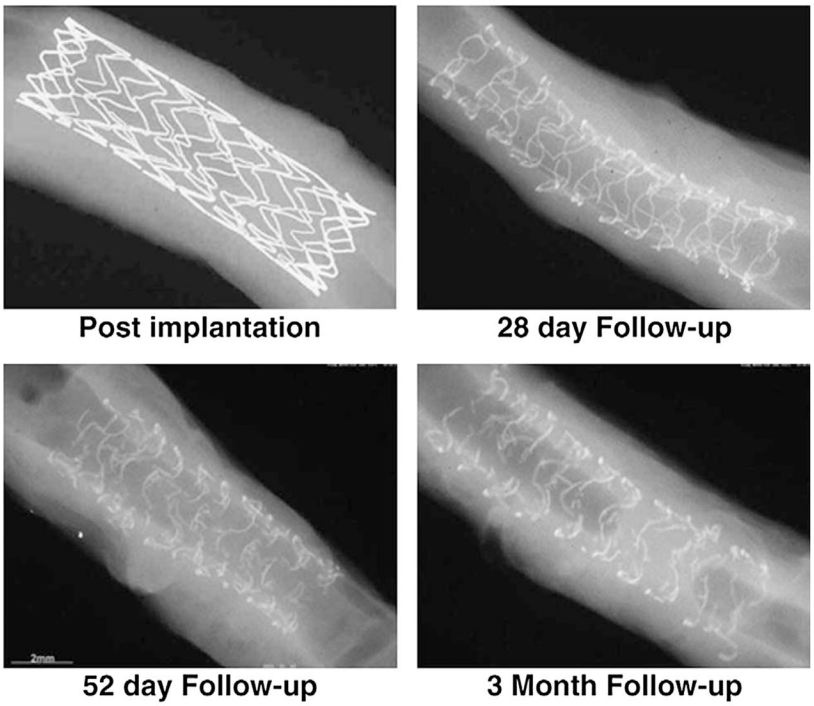

Fig. 1.
Radiography at low-kilovoltage of AMS implanted in porcine coronary arteries[25].

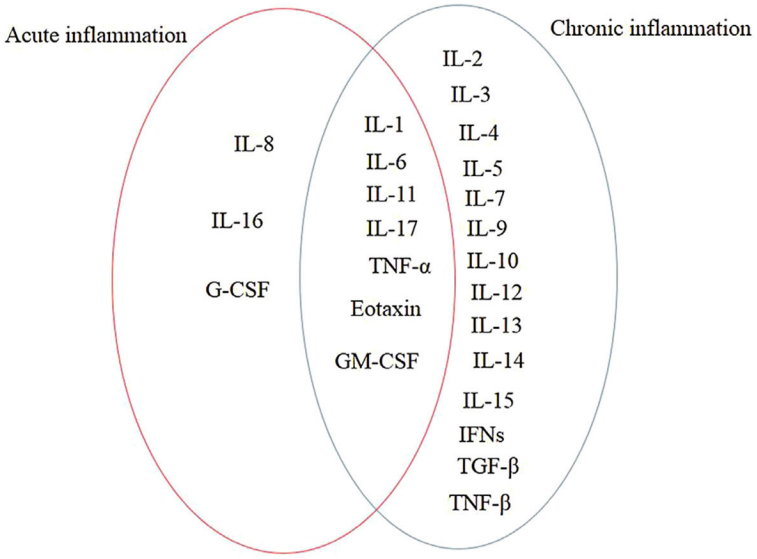

Fig. 2.
Cytokines involved in acute and chronic inflammation reactions[72].

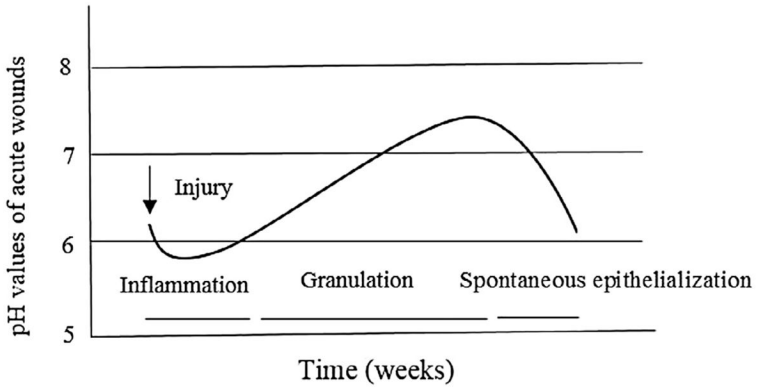

Fig. 3.

pH change during the acute skin wound healing process (adapted from Schneider et al.[102]).

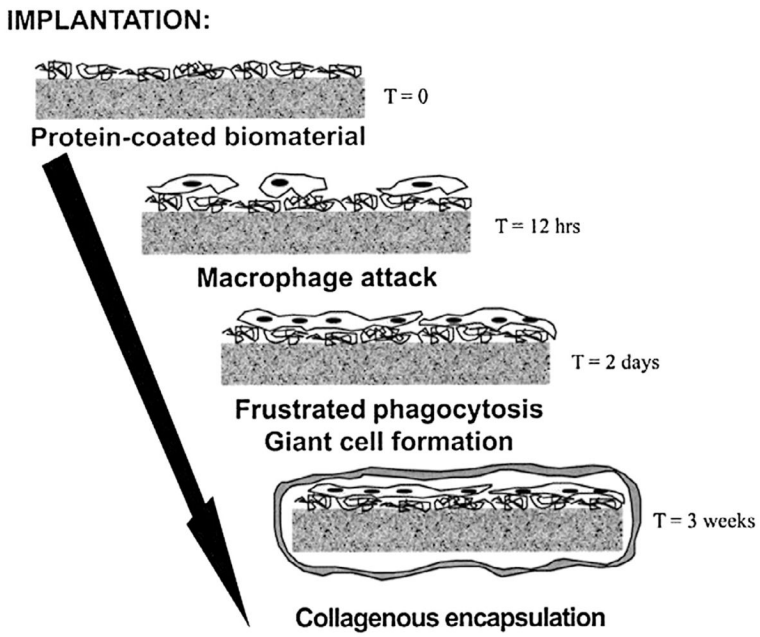

Fig. 4.
Process of fibrosis encapsulation formation[123].

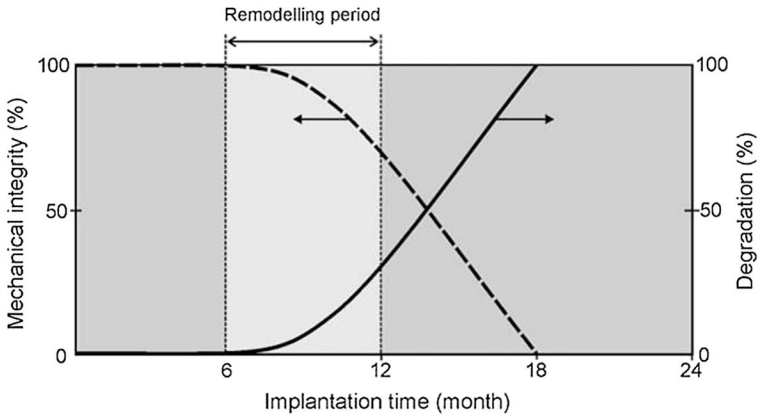

Fig. 5.
Ideal relationship between mechanical integrity and Mg alloy degradation[148].

Table 1

In vitro biocompatibility and hemocompatibility of Mg alloys used for stent applications

Alloy	Cell type	Viability	Hemocompatibility	Culture time (day)	Authors and references
MgCa 0.4%	HUVEC; HUVSMC	<5%; ~90%	–	10	Drynda et al.[6]
MgCa 0.6%		<5%; ~80%			
MgCa 0.8%		<5%; ~90%			
MgCa 1.2%		<5%; ~70%			
MgCa 2.0%		<5%; ~70%			
Mg–Nd–Zn–Zr	HUVEC cell line EA.hy926	10% Extract: ~95%	Hemolysis ratio: 52%	1	Mao et al.[7]
		50% Extract: ~85%			
		10% Extract: ~110%		3	
		50% Extract: ~110%			
		10% Extract: ~ 15%		5	
		50% Extract: ~120%			
Mg3.5Li	HUVEC cell line ECV304; rodent VSMC	~85%; ~135%	Hemolysis ratio: ~3.8%	1	Zhou et al.[8]
		~90%; ~80%	Adhered platelets: ~9000	3	
		~87%; ~80%		5	
Mg8.5Li	HUVEC cell line ECV304; rodent VSMC	~95%; ~200%	Hemolysis ratio: ~3%	1	Zhou et al.[8]
		~80%; ~110%	Adhered platelets: ~9000	3	
		~80%; ~105%		5	
Mg8.5Li1Al	HUVEC cell line ECV304; rodent VSMC	~93%; ~198%	Hemolysis ratio: ~4%	1	Zhou et al.[8]
		~75%; ~100%	Adhered platelets: ~5000	3	
		~90%; ~90%		5	
Mg3.5Li2Al2RE	HUVEC cell line ECV304; rodent VSMC	~80%; ~125%	Hemolysis ratio: ~4.2%	1	Zhou et al.[8]
		~80%; ~75%	Adhered platelets: ~5000	3	
		~90%; ~70%		5	
Mg3.5Li4Al2RE	HUVEC cell line ECV304; rodent VSMC	~80%; ~125%	Hemolysis ratio: ~4.2%	1	Zhou et al.[8]
		~80%; ~90%	Adhered platelets: ~13 000	3	
		~70%; ~90%		5	
Mg8.5Li2Al2RE	HUVEC cell line ECV304; rodent VSMC	~40%; ~105%	Hemolysis ratio:~7.5%	1	Zhou et al.[8]
		~75%; ~75%	Adhered platelets: ~3000	3	

Alloy	Cell type	Viability	Hemocompatibility	Culture time (day)	Authors and references
		~70%; ~70%		5	
WE42	HUVEC	~75%	–	1	Guo et al.[9]
Mg–0.5Sr	HUVEC	~98%	–	1	Bomapour et al.[10]
		~102%		4	
		~112%		7	
WE43	HUVEC	~104%	–	1	Bomapour et al.[10]
		~110%		4	
		~104%		7	
Mg–2.5Nd–0.2Zn–0.4Zr	HUVEC	10% Extract: ~95%	–	1	Mao et al.[11]
		50% Extract: ~90%			
		10% Extract: ~110%		3	
		50% Extract: ~110%			
		10% Extract: ~110%		5	
		50% Extract: ~120%			

Note: HUVEC = human umbilical endothelial cell.

Table 2

In vivo biocompatibility evaluation for Mg alloys used in stent applications

Alloy	Animal type	Implantation time (day)	Inflammation score	Injury score	Neointimal area (mm^2)	Minimal luminal diameter VS benchmark control (mm)	Authors and references
AE21	Domestic pigs, left anterior descending artery	10	–	–	–	3.46 vs 3.36	Heublein et al.[21]
		35	–	–	1.41	1.63 vs 2.59	
		56	–	–	2.71	2.48 vs 2.81	
WE43	Minipigs, coronary artery	30	–	–	–	1.49 vs 1.34	Di Mario et al.[22]
		90	–	–	–	1.68 vs 1.33	
AZ31B	New Zealand white rabbits, distal and proximal infrarenal abdominal aorta	30	1.89 ± 0.76	1.32 ± 0.12	1.44 ± 0.04	–	Li et al.[23]
		60	1.45 ± 0.35	1.54 ± 0.31	1.41 ± 0.08	–	
		90	1.16 ± 0.19	1.68 ± 0.65	1.43 ± 0.02	–	
		120	1.26 ± 0.34	0.79 ± 0.54	1.47 ± 0.03	–	
Sirolimus-eluting AZ31B	–	30	2.26 ± 0.34	1.25 ± 0.13	0.60 ± 0.22	–	
		60	1.65 ± 0.48	1.48 ± 0.26	0.63 ± 0.27	–	
		90	1.35 ± 0.37	1.49 ± 0.35	0.57 ± 0.14	–	
		120	1.31 ± 0.42	1.38 ± 0.35	0.58 ± 0.10	–	
AMS (WE43)	Gottingen minipigs, coronary artery	28	–	0.37 ± 0.72	1.14 ± 0.92	1.51 ± 0.46 vs 1.26 ± 0.41	Loos et al.[17]
		56	–	0.12 ± 0.24	1.23 ± 0.55	1.55 ± 0.51 vs 1.09 ± 0.25	
Magic stent (WE43)	Juvenile domestic crossbred swine	3	–	–	–	–	Waksman et al.[24]
		28	1.89 ± 1.07	1.67 ± 1.13	34 ± 27.8	2.89 ± 0.26 vs 3.06 ± 0.22	
		90	–	0.47 ± 0.33	–	1.58 ± 0.37 vs 1.42 ± 0.56	

Table 3

Clinical trials of Mg-based stents

Trial name	Stent/Alloy	Number of subjects	Symptoms	Summarized outcomes	Authors and references
–	AMS (WE43)	20 (M10, F10)	Critical limb ischemia	One patient died; primary clinical patency 89.5%	Peeters et al.[27]
AMS INSIGHT	AMS (WE43)	117	Critical limb ischemia; de novo stenotic or occlusive atherosclerotic disease	Within 30 days, the amputation or death rate was 5.3% vs 5.0% in control group; the 6-month angiographic patency rate was 31.8% vs 58% in control group; no efficacy in the long-term patency compared to percutaneous transluminal angioplasty (PTA)	Bosiers and Investigators[28]
–	AMS (WE43)	1 female preterm baby	Ligation of the left pulmonary artery	On 7th day, reperfusion of the left lung as complete as vascular system allowed and thrombus distal to the stent was dissolved; after 6 weeks, the patient was extubated; 5 months later, the left lung perfusion persisted with a slight difference in size between left and right pulmonary artery	Zartner et al.[29]
–	AMS (WE43)	A three-week-old male baby	Critical aortic coarctation	At the age of 3 months, ventricular septal defect (VSD) closure had to be performed because of left to right shunting	Schranz et al.[30]
–	Magic stent (WE43)	A two-month old girl	Pulmonary atresia, VSD, and multiple aortopulmonary collaterals with severely hypoplastic pulmonary arteries	Initial significant increase in vessel diameter at first, but significant restenosis occurred at 4 months	McMahon et al.[31]
PROGRESS-AMS	AMS (WE43)	63 (M 44, F19)	Ischemic heart disease or silent ischemia and a discrete de novo lesion in coronary artery	Diameter stenosis reduced from 61.5% ± 13.1% to 12.6 ± 5.6%; in segment acute gain of 1.41 ± 0.46 mm and late loss of 1.08 ± 0.49 mm; 4 months later, ischemia-driven target lesion revascularization rate was 23.8%, the overall target lesion revascularization rate was 45% after 1 year	Erbel et al.[3]
BIOSOLVE-I	Drug-eluting absorbable metal scaffold (DREAMS, WE43)	46	–	2 patients had target lesion failure after 6 months, and at 12 months another patient had same problem; overall target lesion revascularization was 26.7% after 12 months; at 6 months and 12 months, the lumen loss were reduced (0.65 ± 0.50 mm and 0.52 ± 0.39 mm, respectively) compared to 1.08 ± 0.49 mm at 4 months of PROGRESS trial	Haude et al.[4]

Note: M = Male, F = Female.

J Mater Sci Technol. Author manuscript; available in PMC 2017 September 01.